Modelling of food processes under uncertainty

Mechanistic 3D model of chicken meat roasting

Rabeler, Felix; Feyissa, Aberham Hailu

Published in:
Journal of Food Engineering

Link to article, DOI:
10.1016/j.jfoodeng.2019.05.006

Publication date:
2019

Document Version
Peer reviewed version

Accepted Manuscript

Modelling of food processes under uncertainty: Mechanistic 3D model of chicken meat roasting

Felix Rabeler, Aberham Hailu Feyissa

PII: S0260-8774(19)30200-6

DOI: https://doi.org/10.1016/j.jfoodeng.2019.05.006

Reference: JFOE 9596

To appear in: *Journal of Food Engineering*

Received Date: 31 October 2018

Revised Date: 16 March 2019

Accepted Date: 7 May 2019

Please cite this article as: Rabeler, F., Feyissa, A.H., Modelling of food processes under uncertainty: Mechanistic 3D model of chicken meat roasting, *Journal of Food Engineering* (2019), doi: https://doi.org/10.1016/j.jfoodeng.2019.05.006.

Modelling of food processes under uncertainty: Mechanistic 3D model of chicken meat roasting

Felix Rabeler*, Aberham Hailu Feyissa

Food Production Engineering, National Food Institute, Technical University of Denmark (DTU), Denmark

*Corresponding author:

Søltofts Plads, 2800, Kgs. Lyngby, Denmark

Email address: felra@food.dtu.dk, Tel.: +45 45252531

Keywords: Heat and mass transfer, Monte Carlo method, Morris screening, standardized regression coefficients, transport phenomena in porous media, global uncertainty and sensitivity analysis

Abstract

Mathematical models that describe the transport phenomena and quality changes of foods during processing contain several uncertain model input parameters which result in uncertain model predictions. The objective of this study was to evaluate the impact of uncertain input parameters on the model predictions of the mechanistic 3D model of chicken meat roasting and to identify as well as rank the most important model parameters. We found that the uncertainty in the model output variables varies with roasting time, but also among the different output variables, by using the Monte Carlo method. To decompose the variance with

respect to the input parameters, the method of standardized regression coefficients (SRC), a global sensitivity analysis method, was used. Consequently, the uncertain input parameters were ranked according to their relative impact. The results of the SRC method were compared with the Morris screening, a one-step-at-a-time (OAT) global sensitivity analysis method. The comparison of the two applied sensitivity methods showed that the ranking of the input parameters is similar, while the Morris screening is more efficient computational wise. Finally, we illustrate how the results of the analyses can be used for model refinement as well as to highlight parameters and areas where further research is necessary.

1. Introduction

The development of mathematic models to predict the heat and mass transfer during the baking or cooking of foods became an essential research field in food engineering. Models enable enhanced process control and make the scale-up easier. Additionally, the physics and mechanisms inside the foods during processing can be studied in a way that is not possible by experimentation alone (Datta, 2015).

However, mechanistic models that predict the transport phenomena during roasting processes of food products are rather complex. This is due to the highly coupled mechanisms of heat and mass transfer and the resulting physical-chemical changes. These are for example the evaporation of water and the following internal pressure increase, the chemical reactions leading to a browning of the surface or the denaturation of proteins causing a change in the microstructure of the food product. Detailed explanations of different roasting models are given for example by Feyissa et al. (2013) (pork meat roasting); Goñi and Salvadori (2011) (beef meat roasting; Jha (2005) (grain roasting); Rabeler and Feyissa (2018a) (chicken meat roasting) or van der Sman (2007) (beef meat roasting). To model these complex mechanisms many model input parameters and variables are necessary.

In a recent study we presented a mechanistic 3D model for the roasting of chicken breast meat in a convective oven, where the texture profile inside the chicken meat was predicted from the local temperature development with time (Rabeler and Feyissa, 2018a). To describe the transport phenomena and quality changes, approximately 130 input parameters and variables are needed. For chicken breast meat, however, not all input parameters are available that are necessary to describe the heat and mass transfer during the roasting or the values come with a large inherit uncertainty. This is due to the natural variation of the chicken meat tissue, but also from the fact that many phenomena that happen during the roasting are not fully understood. The uncertainties in the input parameters, however, affect the accuracy of the developed model, leading to uncertainties in the model predictions

Uncertainty analysis techniques allow the evaluation of the propagation of uncertainty in the developed model. The impact of the uncertain input parameters on the model predictions can be determined and, consequently, the reliability of the model studied. Sensitivity analysis allows then the decomposition of the obtained variance in the model output in respect to the input parameters. In details, the contribution of each studied input parameter to the output variance is obtained and the parameters can be ranked according to their relative influence on the model output. By running both methods in tandem, the robustness of the developed model can be determined and a fundamental understanding of the relationships between the input parameters and output variables can be achieved (Saltelli, 2006; Sin et al., 2009).

Furthermore, the obtained information from the uncertainty and sensitivity analysis can be used in the following ways: prioritization of further research and experimental work by focusing efforts on parameters that mainly influence the model output; refinement and reduction of the model by describing the most influencing parameters as accurate as possible while fixing parameters with low impact; and for optimization of the studied process by concentrating on the most influencing process settings (Saltelli, 2006; Saltelli et al., 2007).

In food science mainly local sensitivity analysis techniques are applied to study the influence of one uncertain input parameter with small variations around their nominal value on the model predictions (Gulati et al., 2016; Ousegui et al., 2010; Purlis and Salvadori, 2009). Local sensitivity analyzing techniques vary only one input parameter at a time (one-factor-at-a-time, OAT), while the other parameters are kept constant at their nominal value. The corresponding changes of the output variables are then evaluated (Dimov and Georgieva, 2010). This requires relatively low computational effort and is most of the time easy to implement (Feyissa et al., 2012). However, as local sensitivity analysis varies only one parameter at a time, it is not possible to evaluate the effect of the whole uncertain input parameter space on the model predictions or to detect possible interactions between 2 or more uncertain input parameters (Czitrom, 1999).

Global sensitivity techniques, on the contrary, vary all uncertain input parameters at a time. Thus, the impact of all uncertain input parameters, with their corresponding uncertainty range, on the model predictions can be studied (Dimov and Georgieva, 2010). This means, however, that the implementation often takes more time and the computational burden is higher.

In food science only a few authors studied the global uncertainty and sensitivity of mathematical models (e.g. 2D modelling of contact baking process (Feyissa et al., 2012)), while it already became a common routine in other disciplines like for environmental models (Campolongo and Saltelli, 1997), ecological models (Cariboni et al., 2007), wastewater treatment (Sin et al., 2011) or risk assessment (Gargalo et al., 2016).

The objective of this work is, therefore, to study the impact of the uncertain model input parameters on the predictions (temperature, moisture and texture) of the mechanistic 3D model of chicken meat roasting in a convective oven and to identify the parameters with the highest relative impact. Different global sensitivity analysis methods are compared and the impact of the sampling method and size on the sensitivity analysis is studied. The results of

the analyses are then discussed in terms of model refinement and reduction as well as possibilities for process optimization.

2. Methodology

2.1. Modelling the roasting of chicken breast meat

The roasting of chicken breast meat in a convection oven involves coupled heat and mass transfer, with a convective heat flux from the surrounding hot air to the sample surface, internal transfer of the heat by convection and conduction, water migration within the product by diffusion and convection, and evaporation of liquid water from the surface to the surrounding hot air (Rabeler and Feyissa, 2018a).

The governing equations for heat and mass transfer are given by Eq. (1) and Eq. (2), respectively (Bird et al., 2007):

Heat transfer: $$c_{p,cm}\,\rho_{cm}\,\frac{\partial T}{\partial t} = \nabla(k_{cm}\,\nabla T) - \rho_w\,c_{p,w}\,u_w\,\nabla T \quad (1)$$

Mass transfer: $$\frac{\partial C}{\partial t} = \nabla(-D\,\nabla C + C\,u_w) \quad (2)$$

where $c_{p,i}$ is the specific heat capacity (J/(kg K)), ρ_i the density (kg/m^3), k_i is the thermal conductivity (W/(m K)), T is the temperature (K), u_w the fluid velocity (m/s), C the moisture content (kg of water/kg of product), D the water diffusion coefficient (m^2/s) and t the time (s). The main moisture transport inside the chicken breast meat results from a pressure gradient due to protein denaturation and shrinkage of the protein network and is given by Darcy's law in the following form (Eq. (3)) (Rabeler and Feyissa, 2018a):

$$u_w = \frac{-\kappa}{\mu_w}\,\nabla \mathrm{P} \quad (3)$$

with the permeability κ (m^2), the dynamic viscosity of water μ_w (Pa s) and the swelling pressure P (Pa). The boundary conditions for the heat and mass transfer at the boundaries 1, 2, 3 and 6 (see Fig. 1) are described in Eq. (4) and (5):

$$-k_{cm}\nabla T = h\,(T_{air} - T_{surf}) \quad (4)$$

$$-D\,\nabla C + C\,u_w = \beta_{tot}\,(C_{surf} - C_{air}) \quad (5)$$

The heat transfer coefficient (h) at the boundaries 1, 2 and 3 is h_{eff} (combined convective and radiative heat transfer) and at boundary 6 it is h_{bot}. The mass transfer coefficient β_{tot} is described by Eq. (6):

$$\frac{1}{\beta_{tot}} = \frac{1}{\beta_{ext}} + \frac{1}{\beta_{skin}} \quad \text{with} \quad \beta_{skin} = \beta_1\,C^b \quad (6)$$

where β_{ext} is the eternal mass transfer coefficient (m/s), which is calculated with the Lewis relation (Rabeler and Feyissa, 2018a), β_{skin} is another mass transfer coefficient that depends on the moisture content (C) and the two fitting parameters β_1 and b.

The boundaries 4 and 5 are symmetry boundary conditions. For a detailed description of the developed model, the reader is referred to Rabeler and Feyissa (2018a).

The texture changes (hardness and chewiness) of chicken breast meat with temperature and roasting time were described with a modified rate law (Rabeler and Feyissa, 2018b) (Eq. (7)):

$$\frac{\partial Q}{\partial t} = k\,(Q_\infty - Q)^n \quad (7)$$

with the quality attribute Q, the non-zero equilibrium value Q_∞, the reaction order n and the reaction rate constant k ($\text{min}^{-1}\,[\text{Q}]^{1-n}$). The temperature dependency of the reaction rate constant was described with the common Arrhenius equation (Rabeler and Feyissa, 2018b). A detailed description of the model can be found in Rabeler and Feyissa (2018b).

2.2. Model output variables

In total 8 output variables were taken into consideration for the uncertainty and sensitivity analyses as described in section 2.4 and 2.5. The temperature was evaluated at 3 different positions inside the chicken meat sample (see Fig. 1): position A(0,0,1 mm) the bottom temperature (T_A), position B(0,0,10 mm) the core temperature (T_{core}) and position C(0,0,19 mm) the top surface temperature (T_C). Besides the temperature, the volume average moisture content (C_{av}), the moisture content at point A (C_A) and the moisture content at point B (C_B) of chicken meat sample was evaluated as well as the volume average of the texture parameters

hardness (*Ha*) and chewiness (*Cw*) (Rabeler and Feyissa, 2018b). All the selected output variables are represented by the vector Y as: $Y = [T_A, T_{core}, T_C, C_{av}, C_A, C_C, Ha, Cw]$.

2.3. Model input variables

In total 12 uncertain model input parameters were identified, where only a limited amount of data is available, or the values have a large uncertainty. The variation in those uncertain parameters was taken into consideration for the uncertainty and sensitivity analyses. The uncertain input parameters are associated with the following: (1) Initial conditions (T_0 and C_0), (2) boundary conditions (T_{air}, h_{eff}, h_{bot}, C_{air} and b), (3) chicken meat properties (ρ_{cm}, $c_{p,cm}$ and k_{cm}) and (4) transfer coefficients (D and κ). The vector θ represents all the uncertain input parameters, where $\theta = [T_0, C_0, T_{air}, h_{eff}, h_{bot}, C_{air}, b, \rho_{cm}, c_{p,cm}, k_{cm}, D, \kappa]$.

2.4. Uncertainty analysis

The well-established Monte Carlo technique was used in this study to determine the uncertainty in the model outputs resulting from the uncertainty in the model input (Helton, 1993; Metropolis and Source, 1949). The method was chosen as it is computationally effective and reliable (Helton and Davis, 2003; Sin et al., 2009). The Monte Carlo method consists of three steps: (1) identification of uncertain input parameters and specification of the input uncertainty, (2) generation of samples from the input space and (3) model evaluation with sampled input uncertainty with statistical analysis of the results (Feyissa et al., 2012). The individual steps are described in detail in the following sections.

2.4.1. Step 1: Specifying uncertainty in input parameters

The first step, the selection of the uncertainty range of the uncertain input parameters, is the most important step in the Monte Carlo procedure. The uncertainty range was selected after a subjective expert review process of the literature data, experimental data and expert assumptions (Table 1). For the experimental gained input parameters (marked with *) the range from the measurements was taken. For the remaining uncertain input parameters three

classes with low, medium and high uncertainties were defined with 5, 15 and 30 % variability around the mean value, respectively. For the permeability (κ) of meat products only limited knowledge is available in literature. Consequently, the broader range as reported by Datta (2006) and Feyissa et al. (2013) was chosen (see Table 1). For all input parameters a uniform probability distribution within the specified range was assumed.

2.4.2. Step 2: Sampling

Three different sampling methods, the Halton sequence, the Latin hypercube sampling as well as the Sobol sequence were used in this study to evaluate the influence of the sampling method on the standardized regression coefficients (see section 2.5.1). A detailed description of the Halton sequence and Sobol sequence is given by Kocis and Whiten (1997) and for the Latin hypercube sampling by Helton and Davis (2003).

The sampling was performed from the corresponding input parameter intervals (Table 1) which results in a θ_{NxM} sample matrix (Feyissa et al., 2012):

$$\begin{bmatrix} \theta_1 \\ . \\ . \\ \theta_i \\ . \\ . \\ \theta_N \end{bmatrix} = \begin{bmatrix} \theta_{11}, \theta_{21}, \theta_{31}, \dots, \theta_{M1} \\ . \\ . \\ \theta_{1i}, \theta_{2i}, \theta_{3i}, \dots, \theta_{Mi} \\ . \\ . \\ \theta_{1N}, \theta_{2N}, \theta_{3N}, \dots, \theta_{MN} \end{bmatrix} \quad (8)$$

where θ_i is the sample value of the corresponding uncertain input parameter, M is the total number of uncertain input parameters (M = 12 for this study) and N the total number of samples. The sample size in this study (N) was varied from 20 to 1000 samples until it had no further influence on the sensitivity analysis results.

2.4.3. Step 3: Model evaluation and statistical analyses

The obtained matrix, θ_{NxM}, with the sampled input parameters was propagated by performing dynamic simulations for N input samples of M input parameters (each row of θ generated one simulation). The coupled governing equations for heat and mass transfer (a system of partial

differential equations, PDEs) combined with constitutive equations, as well as the ordinary differential equations (ODE) that describe the texture changes of chicken breast meat were solved. The model output variables were stored in the three-dimensional matrix Y_{GxKxN}. The matrix contained for each time instant G (10 s time steps from t=0 to t=600 s) the predictions of the K output variables (8 outputs) for a total number of N samples (Feyissa et al., 2012). The results obtained from the model simulations were then analyzed and the mean as well as the 10th and 90th percentile of the output distributions were calculated for each output variables.

2.5. Global sensitivity analysis

The standardized regression coefficients method (SRC) and the Morris screening were used to evaluate the sensitivity of the uncertain input parameters on the model output variables. The simulation output variables (e.g., temperature, moisture content and texture changes) vary with time (dynamic profile). The sensitivity of the input parameters was, therefore, analyzed at two different time points, t=4 min (heating dominant period) and t=8 min (evaporation dominant period), corresponding to the middle and the end of the roasting process, respectively.

2.5.1. Standardized regression coefficients

The method of standardized regression coefficients (SRC) as described by Helton and Davis (2003) and Sin et al. (2009) was used to evaluate the sensitivity of the uncertain input parameters on the model output variables and to rank the parameters. Using the data from the Monte Carlo simulations (see section 2.4), linear regression models were constructed for every model output variable in Y (see section 2.2) using Eq. (9):

$$\frac{sY_{im}-\mu_{sym}}{\sigma_{sym}} = \sum_{j=1}^{M} \beta_{im} \frac{\theta_{ij}-\mu_{\theta j}}{\sigma_{\theta j}} + \varepsilon_{im} \quad (9)$$

where θ is the vector with the input parameters (see section 2.3), m is the index of the output vector sY, i is the index of the Monte Carlo simulations (samples), j is the index of the input

parameter vector θ, ε is the error of the linear regression model, β_{im} is the standardized regression coefficient (SRC) and M is the total number of uncertain input parameters. For a linear model the following condition holds for the standardized regression coefficient: $\sum_i(\beta_{im})^2 = 1$. In most cases, $\sum_i(\beta_{im})^2 \leq 1$ and it is equal to the coefficient of determination R^2 (Saltelli et al., 2007; Sin et al., 2011). To apply the SRC method, $\sum_i(\beta_{im})^2$ or R^2 should be above the recommended value of 0.7 to ensure a necessarily linear model (Cariboni et al., 2007).

2.5.2. Morris screening

The Morris screening is a one-step-at-a-time (OAT) sensitivity analysis method, which means that only one input parameter is changed at each simulation run. By repeating these local changes for a predefined number of times, a global sensitivity analysis is achieved (Morris, 1991). The method is relatively simple to implement, and the obtained results can be interpreted easily. Furthermore, it is typically computationally efficient compared to other sensitivity analysis methods (i.e. fewer sample numbers needed) (Campolongo and Saltelli, 1997; Saltelli, 2004).

With the Morris method the distribution of the so-called Elementary Effects (*EE*) of the input parameters on the model output variables is estimated. The distribution of the effects of the *jth* model input parameter on the *mth* model output variable is denoted as F_{jm} (Sin et al., 2009). The elementary effects EE_{jm} were estimated using Eq. (10) (Morris, 1991):

$$EE_{jm} = \frac{\partial sY_m}{\theta_j} = \frac{sY_m(\theta_1,\theta_2,\theta_j+\Delta,\ldots,\theta_M) - sY_m(\theta_1,\theta_2,\theta_j,\ldots,\theta_M)}{\Delta} \quad (10)$$

where $sY_m(\theta_1, \theta_2, \theta_j,\ldots, \theta_M)$ is the model output at the input parameters θ_1 to θ_M and $sY_m(\theta_1, \theta_2, \theta_j+\Delta,\ldots, \theta_M)$ is the model output where θ_j is changed by the predetermined perturbation factor Δ.

The range of the input parameters θ is divided into p levels and each input can only take values from these predefined levels. In this study p was set to 8, corresponding to the 12.5th

percentile of the uniform input distributions (Ruano et al., 2011). Thus, the perturbation factor, Δ, had the value of $\Delta = p/(2(p-1)) = 4/7$. The elementary effects, EE_{jm}, were calculated at randomly sampled points in the input space and the procedure repeated for a number of predefined repetitions, r (Sin et al., 2009). By following this one-factor-at-a-time design (OAT), which was proposed by Morris, a total of $r*(M+1)$ model simulations are necessary. In this study, the number of repetitions, r, was increased until it had no further influence on the analysis results. A detailed description of the Morris sampling was given by Sin et al. (2009).

Finally, the means (μ) of the distributions of the calculated elementary effects as well as the standard deviations (σ) were estimated. Both sensitivity parameters were then used to rank the input parameters according to their influence on the model output. The model input parameters with low μ and low σ values can be considered as non-influential on the model outputs (Morris, 1991). Furthermore, the graphical approach as proposed by Morris was used to evaluate the input parameters influence. The mean, μ, and the standard deviation, σ_i, are plotted together with two lines which correspond to $\mu_i = \pm 2sem_i$. The standard error of means (sem) is calculated as $sem_i = \sigma_i/\sqrt{r}$ (Morris, 1991).

2.6. Model implementation and solution

COMSOL Multiphysics® 5.3 with MATLAB® was used to solve the coupled PDEs of heat and mass transfer (see section 2.1) as well as the ODEs of the texture kinetics (see section 2.1), and to perform the uncertainty and sensitivity analysis.

3. Results and discussion

3.1. Uncertainty in the model outputs

The results of the uncertainty analysis are presented for the Halton sequence sampling method with a sample size of $N = 500$ samples (see section 3.2). From the raw data obtained by the Monte Carlo simulations, the mean 10^{th} and 90^{th} percentile was calculated for every model

output variable at each time point. Fig. 2, 3 and 4 present the results for the temperature, moisture and texture output variables, respectively. A higher band or spread in the distribution can be related directly to a higher uncertainty in the model prediction.

The temperature profiles at the position A (close to the bottom), T_A, and at position C (close to the surface), T_C, show a similar trend (Fig. 2a and 2c, respectively). At the start of the cooking process, the uncertainties in the temperature predictions are increasing with time (heating dominant region), while they are decreasing again when the temperature is leveling off around the boiling temperature of water (evaporation dominant region). The heat transfer at the bottom of the chicken meat (in contact with roasting plate) is higher compared to the surface and, consequently, T_A is increasing faster than T_C. Accordingly, the lowest uncertainty for T_A was found after 6 min of roasting, while for T_C the evaporation dominant region is just reached at the end of the process (after 10 min of roasting) (Fig. 2a and 2c, respectively). The uncertainty of the core temperature predictions (T_{core}), on the contrary, is increasing over the whole roasting time, with the highest uncertainty at the end of the process (Fig. 2b).

For the average moisture content of the chicken meat sample (C_{av}) the band for the uncertainty stays constant during the whole roasting process (Fig. 3a). A similar trend was found for the moisture content profile close to the surface (C_C) (Fig. 3c). For the moisture content close to the bottom (C_A) the spread and, consequently, the uncertainty is increasing towards the end of the roasting process (Fig. 3b).

The texture parameters hardness (*Ha*) and chewiness (*Cw*) are a function of the temperature development in the center part of the chicken meat sample (see striped part in Fig.1). In the beginning of the roasting process the temperature is below the denaturation temperature of the proteins and, therefore, no change of *Cw* and *Ha* can be observed (Fig. 4a and 4b). With increasing roasting time, the temperature is rising inside the sample and, consequently, the texture parameters are increasing with time. In the beginning of the roasting process, chewiness (*Cw*) is more sensitive to the temperature changes (higher activation energy

(Rabeler and Feyissa, 2018b)) and, therefore, it starts to rise earlier compared to the hardness (*Ha*) (lower activation energy). The uncertainty for chewiness is first increasing with time where after it is decreasing and levelling off again when the equilibrium value of this texture parameter is reached (Fig. 4b). After the texture parameter hardness starts to rise (approximately after 3.5 min), a constant uncertainty (band) was found along the roasting process (Fig, 4a).

3.2. Standardized regression coefficient (SRC) for global sensitivity analysis

A linear regression model was constructed for each model output variable (sY_i), by using the linear least square method, and the corresponding SRC coefficients were obtained at different time points (t=4 min and t = 8 min, see section 2.5). As a first step, the influence of the sampling method (Latin hypercube sampling, Sobol sequence and Halton sequence (see section 2.4.2)) as well as the sample number (N) on the standardized regression coefficients was studied. For clarity only the influence of the oven temperature (T_{oven}) on the SRC value of the core temperature (T_{core}) at the roasting time of 8 min is reported.

The impact of the sampling method and the sampling size and on the SRC value is shown in Fig. 5. For low sample numbers (20 to 100) a high discrepancy between the sampling methods can be seen, especially between the Halton and Sobol sequence. However, with increasing sample size the SRC value is reaching a constant value (dashed line in Fig. 5) faster for the Halton and Sobol sequence (N = 500) compared to the Latin hypercube sampling method (N = 1000). This shows that the Halton and Sobol sequence are computationally more efficient and should, therefore, be used instead of the Lating hypercube sampling. Accordingly, the further analyses are presented for the Halton sequence with a sample size of 500.

Table 2, 3 and 4 present the results of the SRC method for the temperature, moisture and texture output variables, respectively. Only the first 6 top input parameters that had the highest impact on the model outputs are reported here for clarity.

For all output variables the coefficient of determination, R^2, was found to be higher than 0.92, showing that a necessary degree of linearization was obtained. Therefore, the obtained SRC values can be used to evaluate the impact of the uncertainty in the input parameters (θ) on the output variables (sY) (see section 2.5.1).

The absolute SRC value shows directly the relative impact of the corresponding input parameter on the output variable, while a positive SRC value indicates a positive correlation and a negative SRC value indicates a negative correlation between model input and output.

3.2.1. Chicken meat temperature

After 4 minutes of roasting the temperatures close to the bottom, T_A, and close to the surface, T_C, are most sensitive to the oven temperature, T_{oven}, and the heat transfer coefficients (fan speeds), h_{bot} and h_{eff} (see Table 2). The positive SRC values indicate that higher oven temperatures and fan speeds lead to an increase of both the surface and the bottom temperature. This is reasonable as with a higher oven temperature and heat transfer coefficient, the heat flux from the surrounding hot air to the chicken meat surface is increasing, leading to the rise of the surface and bottom temperature (see Eq. (4)). Towards the end of the roasting process (t = 8 min) the parameters that are correlated to the moisture transport (κ) and evaporation (b) become more important. At this time point both temperatures reached the boiling temperature of water (around 100 °C, see Fig. 2a and 2c), and, therefore, the temperature is mainly controlled by the evaporation of the water from the surface of the chicken sample.

The core temperature, T_{core}, of the chicken meat sample is also most sensitive to the oven temperature, T_{oven}, with positive SRC values (positive correlation). The thermo-physical properties k_{cm} and $c_{p,cm}$ are ranked on the 2nd and 3rd rank, respectively. The SRC values for the thermal conductivity k_{cm} are positive, indicating the positive correlation between k_{cm} and T_{core}. This is reasonable as the thermal conductivity gives the rate of the heat transfer inside the chicken meat. This means that higher values of k_{cm} lead to a faster heat transfer and,

consequently, a faster increase of the core temperature. The specific heat capacity, on the contrary, has a negative impact on the core temperature (negative SRC values). This means, that for lower values of $c_{p,cm}$, less heat is needed to increase the temperature of the chicken sample and, consequently, also the core temperature is rising faster.

3.2.2. Chicken meat moisture content

The ranking of the input parameters according their relative impact on the average moisture content (C_{av}), as well as the moisture contents at the positions A and C (C_A and C_C, respectively) is presented in Table 3 for the two time points of 4 and 8 min.

The average moisture content, C_{av}, is most sensitive to the initial moisture content (C_0) of the sample at both roasting time points. Higher values of C_0 directly result in higher values of C_{av}. The oven temperature (T_{oven}) and fan speed (h_{eff}) are at the second and third position in the ranking, respectively, both having a negative impact on C_{av}. This is reasonable, since increasing values of T_{oven} and h_{eff} lead to an increase in the evaporation of water from the sample surface, which results in the decrease of C_{av}.

After 4 min of roasting, the moisture content close to the top and bottom surface, C_C and C_A, respectively, are most sensitive to the initial moisture content C_0, followed by the permeability κ of the chicken meat, the oven temperature T_{oven} and the heat transfer coefficient (h_{eff} for C_C and h_{bot} for C_A) (Table 3). At 8 min, the moisture content close to the bottom, C_A, is most sensitive to the process parameters T_{oven} and h_{bot}., while the top surface moisture content, C_C, is mainly influenced by the permeability (κ) and the initial moisture content (C_0).

Overall, it becomes clear that the moisture content development is highly influenced by the initial moisture content of the raw chicken breast meat. It is, therefore, necessary to accurately measure the moisture content of the chicken meat sample before the roasting to get an accurate model prediction of the moisture profile during the roasting process. Furthermore, the results show that the permeability of the chicken meat is an important parameter that

should be described as accurate as possible. However, for meat products there are no studies available that show the change of the permeability of meat products during the heating process. Therefore, in future works an experimental study is needed that develops the relationship between the permeability changes as function of the process conditions. A possibility could be to describe this relationship with a variable in Eq. (3) (Darcy's law) that is dependent on the local temperature or moisture content. Thus, the denaturation of proteins and the resulting shrinkage of the protein network during the roasting process would be taken into account and a more accurate model prediction could be obtained.

3.2.3. Chicken meat texture

The texture changes inside the chicken meat sample are a result of protein denaturation and, therefore, they are highly dependent on the temperature development with time. This is highlighted in Table 4, where the 3 top ranked input parameters T_{oven}, $c_{p,cm}$ and k_{cm} are the same as for the core temperature, T_{core} (see Table 3). The thermo-physical properties have again a high impact on the output variables of hardness and chewiness. This underlines the fact that both parameters should be defined as accurate as possible to reduce the uncertainty in the model predictions (model refinement, see section 3.3.2).

The results in Table 4 also show, that from the possible oven settings, the oven temperature (T_{oven}) and fan speed (h_{eff}) have the highest impact on the texture of the chicken meat sample. Therefore, these two parameters can be used to optimize the roasting process with the aim of the optimum texture of the final product for the consumer.

3.3. Morris screening for global sensitivity analysis

The number of repetitions, *r*, was increased from 10 to 50 in order to study its influence on the Elementary Effects, *EE* (see section 2.5.2). We found that 30 repetitions are enough to ensure that it has no further impact on the analysis results. Thus, a total number of 390 simulation runs ($r^*(M+1)$, see section 2.5.2) were necessary. Consequently, the Morris

screening needs 110 simulation runs less than the SRC method (500 samples needed, see section 3.2). One simulation run took around 12 minutes (at the central DTU HPC cluster, with 1 node and 20 cores), which means that the Morris method needed around 1320 minutes less compared to the SRC method.

The visual results of the Morris method at the roasting time of 8 min are presented in Fig. 6. The two lines in the graphs correspond to $\mu_i = \pm 2sem_i$ (see section 2.5.2). Parameters with a low mean and standard deviation value have a low influence on the corresponding output variable, while high means and standard deviations show a high impact. All parameters have a non-linear effect on the model outputs as none of the input parameters have a zero standard deviation together with a non-zero mean.

The ranking of the first six model input parameters (for clarity) according to their impact on the model outputs after 8 min of roasting (t = 8 min) is presented in Table 5. A higher mean value shows a more significant influence of the input parameter on the model output. Furthermore, a positive sign of the mean indicates a positive effect of the input parameter on the output and a negative sign a negative effect.

The ranking of the input parameters according to their impact on the model outputs are mostly in agreement with the results/ ranking of the SRC method. However, there are small differences in the exact order of the parameters for nearly all output variables. Only the ranking for the moisture content at position A, C_A, is the same (compare Table 2 to 4 and Table 5). For the chicken meat temperatures, for example, the order of the thermal conductivity, k_{cm}, and the specific heat capacity, $c_{p,cm}$, are changed in comparison to the SRC ranking. However, there is only a small difference between their mean and SRC values, indicating/showing that the impact of these two thermo-physical properties on the model outputs is not significantly different. Accordingly, the exact order of the two parameters is not influencing the conclusions of their effect on the model predictions.

All in all, the Morris method showed a mostly similar ranking of the input parameters, confirming the results of the SRC method. In this study less samples were needed for the Morris screening which resulted in lower computational cost compared to the SRC method. However, it should be noticed that with an increasing number of input parameters also the needed number of samples is increasing (see section 2.5.2), while the SRC method is independent of the amount of model inputs (Sin et al., 2009).

3.4. Model refinement and perspective

The results from the sensitivity analysis can be used to refine and strengthen the developed model in order to improve the accuracy of the model predictions.

As shown in Table 2, the temperatures at all presented positions (T_A, T_{core} and T_C) as well as the texture parameters (*hardness* and *chewiness*) are highly sensitive to the thermo-physical properties of chicken breast meat ($c_{p,cm}$ and k_{cm}) at both time steps (4 and 8 min). Therefore, both parameters should be refined to decrease the uncertainty on the output parameters.

From literature it is known that both parameters change with temperature, sample composition and fiber direction (Choi and Okos, 1986). Therefore, one way to refine the model could be to include both parameter as function of temperature and composition instead of fixed values. As it can be seen in Fig. 7, it was possible to reduce the uncertainty of the core temperature development by replacing the fixed values of $c_{p,cm}$ and k_{cm} (red dashed lines in Fig. 7) with expressions as function of temperature and composition (blue dashed lines in Fig. 7).

This shows the strength of the uncertainty and sensitivity analysis, where two parameters were identified as highly sensitive to the model output and consequently the model was refined to decrease the uncertainty in the model predictions.

Furthermore, the moisture content of the sample is highly influenced by the permeability κ of the chicken breast meat (Table 3). Higher values of the permeability describe lower resistance to the water flux through the porous medium and, consequently, also an increased water flux towards the surfaces of the chicken meat sample. On the contrary, the uncertainty in the

diffusion coefficient, D, has no significant influence (not shown in Table 3) on the moisture content. This is reasonable as the main moisture transport inside the chicken sample is pressure driven as a result of protein denaturation and the decrease of the water holding capacity (Rabeler and Feyissa, 2018a). The results show that further research is necessary to gain a quantitative knowledge about the change of the permeability with roasting time (i.e. $\kappa(T)$) as already highlighted by different researchers (Feyissa et al., 2013; van der Sman, 2013). On the contrary, for the diffusion coefficient D it is enough to use a constant parameter value (not changing with time) without losing information about the total moisture flux or increasing the uncertainty of the model.

Conclusion

In this study, the impact of uncertain input parameters on the model predictions of the mechanistic 3D model of chicken breast roasting was studied and the most important model parameters were identified, using global uncertainty and sensitivity analysis methods.

The Monte Carlo procedure was effectively applied to evaluate the impact of the uncertainty in the input parameters on the model predictions for the temperature, texture and moisture development. It was found that the uncertainty in the model output variables varies with time, but also among the different output variables. By applying the method of standardized regression coefficients (SRC), a global sensitivity analysis technique, the input parameters with relatively high and low impact on the model predictions were identified and ranked, accordingly. We found that the sampling method and the total number of samples had an influence on the SRC method. The ranking of the input parameters then showed that the roasting is mainly influenced by the oven parameters, the thermo-physical properties and the initial properties of the chicken meat.

The SRC method was afterwards compared with the Morris screening, which confirmed the obtained results (mostly similar ranking of the input parameters). However, for the Morris

method fewer samples were needed showing that in this study it is computationally more efficient.

Overall, the presented uncertainty and sensitivity analysis methods are strong tools to evaluate mechanistic models. They not only ensure the reliability and accuracy of the developed model but inform the operator/ manufacturer about the influence of the process parameters on the safety and quality of the final product.

Nomenclature

a_w	water activity
b	evaporation parameter
C	mass concentration (kg/kg)
c_p	specific heat capacity (J/(kg K))
Cw	chewiness (N)
D	diffusion coefficient (m^2/s)
EE	Elementary Effect
F	distribution of Elementary Effects
G'	storage modulus (Pa)
h	heat transfer coefficient ($W/(m^2 K)$)
Ha	hardness (N)
k	thermal conductivity (W/(m K))
T	temperature (K)
t	time (min)
u	velocity (m/s)
sY	output variable (vector)
Greek symbols	
β	mass transfer coefficient (m/s)
ε_{im}	the error of the regression model
κ	permeability (m^2)
ρ	Density (kg/m^3)
θ	uncertain input parameters (vector)
μ	Mean of observed Elementary Effects
σ	Standard deviation of Elementary Effects
Δ	perturbation factor
Subscripts	
0	initial condition (at t = 0 min)
bot	bottom
cm	chicken meat
eq	equilibrium
ext	external
i	index of Monte Carlo simulations (vector)
j	index of the parameter vector
m	index of output vector
surf	surface
w	water
eff	effective

References

Bird, R.B., Stewart, W.E., Lightfoot, E.N., 2007. Transport Phenomena, Revised 2n. ed. John Wiley & Sons, Inc.

Campolongo, F., Saltelli, A., 1997. Sensitivity analysis of an environmental model : an application of different analysis methods. Reliab. Eng. Syst. Saf. 57, 49–69.

Cariboni, J., Gatelli, D., Liska, R., Saltelli, A., 2007. The role of sensitivity analysis in ecological modelling. Ecol. Modell. 203, 167–182. https://doi.org/10.1016/j.ecolmodel.2005.10.045

Choi, Y., Okos, M.R., 1986. Effects of temperature and composition on the thermal properties of foods. Food Eng. Process Appl. 93–101.

Datta, A.K., 2015. Toward Computer-Aided Food Engineering: Mechanistic Frameworks for Evolution of Product, Quality and Safety During Processing. J. Food Eng. 176, 9–27. https://doi.org/10.1016/j.jfoodeng.2015.10.010

Datta, A.K., 2006. Hydraulic Permeability of Food Tissues. Int. J. Food Prop. 9, 767–780. https://doi.org/10.1080/10942910600596167

Feyissa, A.H., Gernaey, K. V., Adler-Nissen, J., 2013. 3D modelling of coupled mass and heat transfer of a convection-oven roasting process. Meat Sci. 93, 810–820. https://doi.org/10.1016/j.meatsci.2012.12.003

Feyissa, A.H., Gernaey, K. V., Adler-Nissen, J., 2012. Uncertainty and sensitivity analysis: Mathematical model of coupled heat and mass transfer for a contact baking process. J. Food Eng. 109, 281–290. https://doi.org/10.1016/j.jfoodeng.2011.09.012

Feyissa, A.H., Gernaey, K. V., Ashokkumar, S., Adler-Nissen, J., 2011. Modelling of coupled heat and mass transfer during a contact baking process. J. Food Eng. 106, 228–235. https://doi.org/10.1016/j.jfoodeng.2011.05.014

Gargalo, C.L., Cheali, P., Posada, J.A., Gernaey, K. V, Sin, G., 2016. Economic Risk Assessment of Early Stage Designs for Glycerol Valorization in Biorefinery Concepts.

Ind. Eng. Chem. Res. https://doi.org/10.1021/acs.iecr.5b04593

Goñi, S.M., Salvadori, V.O., 2011. Kinetic modelling of colour changes during beef roasting. Procedia Food Sci. 1, 1039–1044. https://doi.org/10.1016/j.profoo.2011.09.155

Helton, J.C., 1993. Uncertainty and sensitivity analysis techniques for use in performance assessment for radioactive waste disposal. Reliab. Eng. Syst. Saf. 42, 327–367.

Helton, J.C., Davis, F.J., 2003. Latin hypercube sampling and the propagation of uncertainty in analyses of complex systems. Reliab. Eng. Syst. Saf. 81, 23–69. https://doi.org/10.1016/S0951-8320(03)00058-9

Jha, S.N., 2005. Mathematical simulation of roasting of grain. J. Food Eng. 71, 304–310. https://doi.org/10.1016/j.jfoodeng.2005.03.006

Kocis, L., Whiten, W.J., 1997. Computational Investigations of Low- Discrepancy Sequences. ACM Trans. Math. Softw. 23, 266–294. https://doi.org/10.1145/264029.264064

Metropolis, N., Source, S.U., 1949. The Monte Carlo Method. J. Am. Stat. Assoc. 44.

Morris, M.D., 1991. Factorial Samplig Plans for Preliminary Computational Experiments. Technometrics 33.

Ngadi, M., Dirani, K., Oluka, S., 2006. Mass Transfer Characteristics of Chicken Nuggets. Int. J. Food Eng. 2. https://doi.org/10.2202/1556-3758.1071

Rabeler, F., Feyissa, A.H., 2018a. Modelling the transport phenomena and texture changes of chicken breast meat during the roasting in a convective oven. J. Food Eng. 237, 60–68. https://doi.org/10.1016/j.jfoodeng.2018.05.021

Rabeler, F., Feyissa, A.H., 2018b. Kinetic Modeling of Texture and Color Changes During Thermal Treatment of Chicken Breast Meat. Food Bioprocess Technol. 1–10. https://doi.org/10.1007/s11947-018-2123-4

Ruano, M. V., Ribes, J., Ferrer, J., Sin, G., 2011. Application of the Morris method for screening the influential parameters of fuzzy controllers applied to wastewater treatment plants. Water Sci. Technol. 63, 2199–2206. https://doi.org/10.2166/wst.2011.442

Saltelli, A., 2006. The critique of modelling and sensitivity analysis in the scientific discourse . An overview of good practices. European Commmission - Joint Research Center, Luxembourg: Office for Official Publications of the European Communities.

Saltelli, A., 2004. Sensitivity analysis in practice: a guide to assessing scientific models (Google eBook).

Saltelli, A., Ratto, M., Andres, T., Campolongo, F., Cariboni, J., Gatelli, D., Saisana, M., Tarantola, S., 2007. Global Sensitivity Analysis. The Primer. John Wiley & Sons, Ltd, Chichester, UK. https://doi.org/10.1002/9780470725184

Sin, G., Gernaey, K. V., Lantz, A.E., 2009. Good Modeling Practice for PAT Applications : Propagation of Input Uncertainty and Sensitivity Analysis. Biotechnol. Prog. 1–12. https://doi.org/10.1021/bp.166

Sin, G., Gernaey, K. V., Neumann, M.B., van Loosdrecht, M.C.M., Gujer, W., 2011. Global sensitivity analysis in wastewater treatment plant model applications: Prioritizing sources of uncertainty. Water Res. 45, 639–651. https://doi.org/10.1016/j.watres.2010.08.025

van der Sman, R.G.M., 2013. Modeling cooking of chicken meat in industrial tunnel ovens with the Flory-Rehner theory. Meat Sci. 95, 940–957. https://doi.org/10.1016/j.meatsci.2013.03.027

van der Sman, R.G.M., 2007. Moisture transport during cooking of meat: An analysis based on Flory-Rehner theory. Meat Sci. 76, 730–738. https://doi.org/10.1016/j.meatsci.2007.02.014

560 **Table 1: Uncertainty ranges for the input parameters**

Parameter	Unit	Nominal value	Source	Range	
				Minimum	Maximum
T_0^*	K	277	(a)	275	283
C_0^*	kg/kg	0.77	(a)	0.73	0.81
T_{oven}^{**}	K	503	(a)	478	528
h_{eff}^{***}	W/(m^2 K)	40	(a)	34	46
h_{bot}^{***}	W/(m^2 K)	55	(a)	49.5	60.5
C_{air}^*	kg/kg	0.05	(a)	0.01	0.1
b^{***}	-	4	(e)	3.4	4.6
ρ_{cm}^{**}	kg/m^3	1050	(b)	997.5	1102.5
$c_{p,cm}^{**}$	J/(kg K)	3591	(b)	3411	3771
k_{cm}^{**}	W/(m K)	0.54	(b)	0.51	0.57
κ	m^2	1x10^{-17}	(c)	1x10^{-18}	1x10^{-16}
D^{****}	m^2/s	3x10^{-10}	(d)	2x10^{-10}	4x10^{-10}

561 Source: (a) measured; (b) calculated from Choi and Okos (1986); (c) obtained from Datta (2006) and Feyissa et
562 al. (2013); (d) obtained from Ngadi et al. (2006); (e) obtained from van der Sman (2013).
563 * Obtained from measurement; ** ± 5 % of the nominal value; *** ± 15 % of the nominal value; **** ± 30 % of
564 the nominal value.
565
566
567
568
569
570
571
572
573
574
575
576

Table 2: Standardized regression coefficients (SRC): ranking of the input parameters according their relative impact on the sample temperatures T_A, T_{core} and T_C for the two time points of 4 and 8 minutes (only the 6 highest ranked input parameters are presented for clarity)

Rank	T_A		T_{Core}		T_C	
	Time Parameter	**4 min** SRC	Time Parameter	**4 min** SRC	Time Parameter	**4 min** SRC
1	T_{oven}	0.756	T_{oven}	0.541	T_{oven}	0.679
2	h_{bot}	0.461	k_{cm}	0.420	h_{eff}	0.628
3	k_{cm}	-0.196	$c_{p,cm}$	-0.417	k_{cm}	-0.174
4	$c_{p,cm}$	-0.179	T_0	0.331	$c_{p,cm}$	-0.153
5	T_0	0.118	h_{eff}	0.274	b	0.130
6	ρ_{cm}	-0.058	ρ_{cm}	-0.269	T_0	0.119
	R^2	0.958	R^2	0.997	R^2	0.996
	Time Parameter	**8 min** SRC	Time Parameter	**8 min** SRC	Time Parameter	**8 min** SRC
1	T_{oven}	0.648	T_{oven}	0.604	T_{oven}	0.664
2	κ	-0.352	k_{cm}	0.405	h_{eff}	0.511
3	h_{bot}	0.339	$c_{p,cm}$	-0.387	κ	-0.314
4	b	0.239	h_{eff}	0.362	k_{cm}	0.193
5	k_{cm}	0.196	ρ_{cm}	-0.252	b	0.173
6	$c_{p,cm}$	-0.154	h_{bot}	0.140	$c_{p,cm}$	-0.151
	R^2	0.949	R^2	0.995	R^2	0.978

Table 3: Standardized regression coefficients (SRC): ranking of the input parameters according their relative impact on the sample moisture contents C_{av}, C_A and C_C for the two time points of 4 and 8 minutes (only the 6 highest ranked input parameters are presented for clarity)

Rank	C_{av}		C_A		C_C	
	Time Parameter	**4 min** SRC	Time Parameter	**4 min** SRC	Time Parameter	**4 min** SRC
1	C_0	0.945	C_0	0.757	C_0	0.583
2	T_{oven}	-0.244	κ	-0.456	κ	-0.465
3	h_{eff}	-0.145	T_{oven}	-0.322	T_{oven}	-0.438
4	b	0.072	h_{bot}	-0.174	h_{eff}	-0.363
5	k_{cm}	0.067	k_{cm}	0.054	k_{cm}	0.108
6	κ	-0.066	$c_{p,cm}$	0.048	$c_{p,cm}$	0.092
	R^2	0.998	R^2	0.958	R^2	0.968
	Time Parameter	**8 min** SRC	Time Parameter	**8 min** SRC	Time Parameter	**8 min** SRC
1	C_0	0.680	T_{oven}	-0.713	κ	-0.461
2	T_{oven}	-0.541	h_{bot}	-0.338	C_0	0.417
3	h_{eff}	-0.286	C_0	0.328	T_{oven}	-0.404
4	κ	-0.2510	κ	-0.258	b	0.242
5	k_{cm}	0.146	k_{cm}	0.142	k_{cm}	0.133
6	b	0.133	$c_{p,cm}$	-0.122	$c_{p,cm}$	0.116
	R^2	0.988	R^2	0.974	R^2	0.937

606 **Table 4: Standardized regression coefficients (SRC): ranking of the input parameters according their relative impact**
607 **on the sample texture variables *Ha* and *Chew* for the two time points of 4 and 8 minutes (only the 6 highest ranking**
608 **input parameters are presented for clarity)**

Rank	***Hardness***		***Chewiness***	
	Time Parameter	**4 min** SRC	Time Parameter	**4 min** SRC
1	T_{oven}	0.565	T_{oven}	0.585
2	$c_{p,cm}$	-0.389	$c_{p,cm}$	-0.401
3	k_{cm}	0.381	k_{cm}	0.399
4	T_0	0.281	h_{eff}	0.285
5	h_{eff}	0.244	T_0	0.279
6	h_{bot}	0.225	ρ_{cm}	-0.233
	R^2	0.924	R^2	0.984
	Time Parameter	**8 min** SRC	Time Parameter	**8 min** SRC
1	T_{oven}	0.614	T_{oven}	0.614
2	k_{cm}	0.396	$c_{p,cm}$	-0.380
3	$c_{p,cm}$	-0.378	h_{eff}	0.366
4	h_{eff}	0.329	k_{cm}	0.357
5	ρ_{cm}	0.242	ρ_{cm}	-0.220
6	T_0	0.206	T_0	0.115
	R^2	0.997	R^2	0.955

609

610

611

Table 5: Morris screening: ranking of the input parameters according to their estimated means of the Elementary Effects distribution.

Rank	T_A		T_{core}		T_C		C	
	Time Parameter	**8 min** μ_i	Time Parameter	**8 min** μ_i	Time Parameter	**8 min** μ_i	Time Parameter	**8 min** μ_i
1	T_{oven}	0.768	T_{oven}	0.583	T_{oven}	0.641	C_0	0.623
2	h_{bot}	0.384	$c_{p,cm}$	-0.366	h_{eff}	0.535	T_{oven}	-0.486
3	κ	-0.377	h_{eff}	0.353	κ	-0.318	κ	-0.269
4	b	0.206	k_{cm}	0.329	$c_{p,cm}$	-0.162	h_{eff}	-0.264
5	k_{cm}	0.184	ρ_{cm}	0.222	k_{cm}	0.162	k_{cm}	0.115
6	$c_{p,cm}$	-0.183	h_{bot}	0.127	b	0.154	b	0.114

Rank	C_A		C_C		*hardness*		*chewiness*	
	Time Parameter	**8 min** μ_i	Time Parameter	**8 min** μ_i	Time Parameter	**8 min** μ_i	Time Parameter	**8 min** μ_i
1	T_{oven}	-0.596	κ	-0.422	T_{oven}	0.590	T_{oven}	0.585
2	C_0	0.309	C_0	0.340	$c_{p,cm}$	-0.360	h_{eff}	0.370
3	h_{bot}	-0.263	T_{oven}	-0.309	h_{eff}	0.323	$c_{p,cm}$	-0.343
4	κ	-0.246	b	0.151	k_{cm}	0.318	k_{cm}	0.320
5	k_{cm}	0.099	k_{cm}	0.082	ρ_{cm}	-0.210	ρ_{cm}	-0.208
6	$c_{p,cm}$	0.072	$c_{p,cm}$	0.048	T_0	0.197	T_0	0.125

Figure captions:

Figure 1: Schematic illustration of the geometry that was used in the model.

Figure 2: Uncertainty of the predicted temperature development using mean, 10^{th} and 90^{th} percentile: a) bottom temperature (position A), b) core temperature (position B) and c) surface temperature (position C). The 500 Monte Carlo simulations are shown in grey.

Figure 3: Uncertainty of the predicted moisture content development using mean, 10th and 90th percentile: a) average moisture content, b) moisture content close to the bottom (position A) and c) moisture content close to the surface (position C). The 500 Monte Carlo simulations are shown in grey.

Figure 4: Uncertainty of the predicted development of the texture parameters a) hardness (*Ha*) and b) chewiness (*Cw*) using mean, 10th and 90th percentile. The 500 Monte Carlo simulations are shown in grey.

Figure 3: Influence of the different sampling methods (Latin hypercube sampling, Halton sequence and Sobol sequence) and the sampling size on the resulting SRC value (input parameter: oven temperature T_{oven}; output variable: core temperature T_{core}) at the roasting time of 8 min. The dashed line shows the mean SRC value after 1000 simulations using the Halton sequence.

Figure 6: Mean (μ_i) and standard deviation (σ) of the Elementary Effects distribution of the model input parameters (in total 12 parameters symbolized as crosses with names) on the model outputs. The two lines in each of the plots correspond to $\mu_i = \pm 2sem_i$.

Figure 7: Uncertainty of the predicted temperature development at the core with fixed values of $c_{p,cm}$ and k_{cm} (red dashed lines) and with $c_{p,cm}$ and k_{cm} as function of temperature and composition (blue dashed lines).

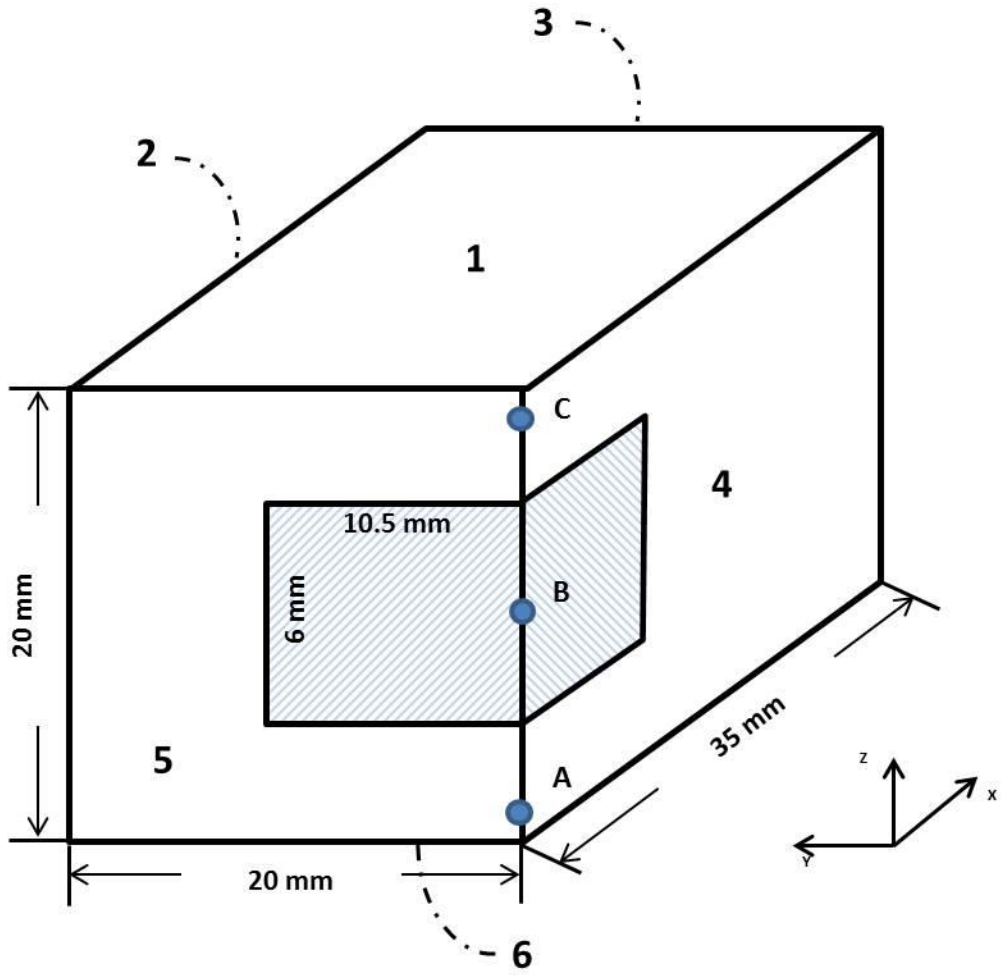

Figure 1: Schematic illustration of the geometry that was used in the model.

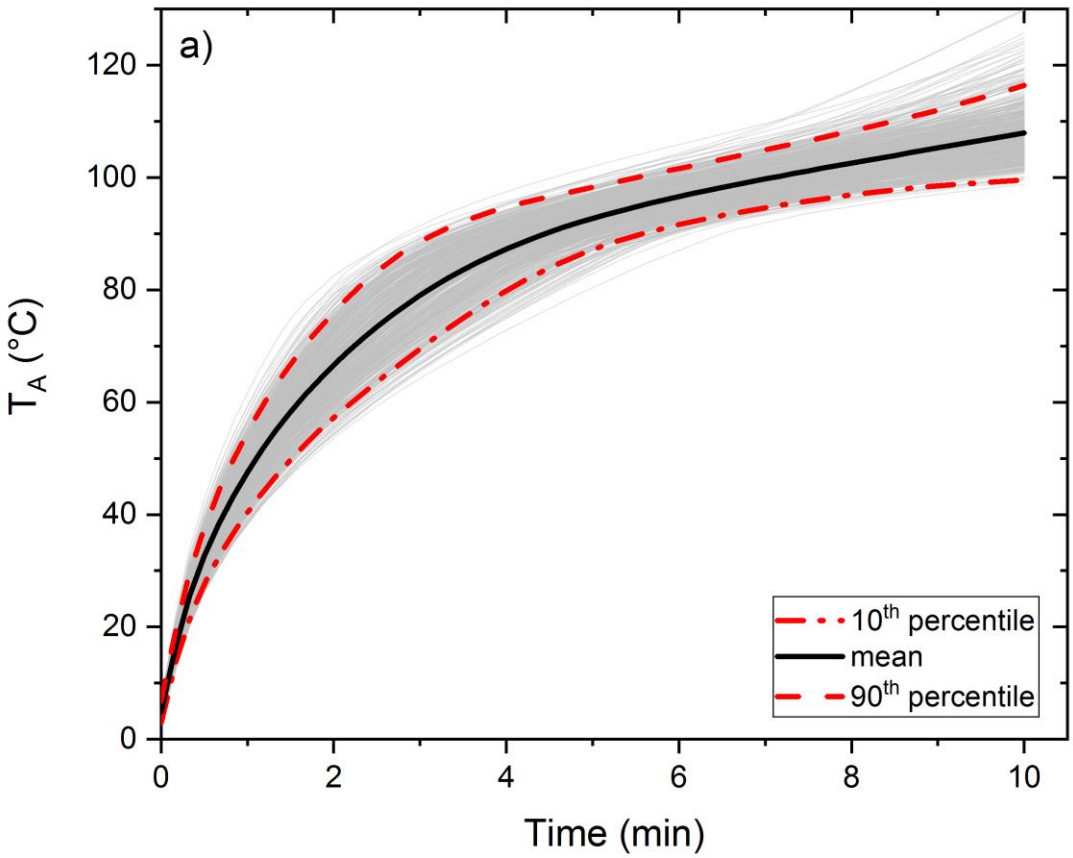

Figure 2: Uncertainty of the predicted temperature development using mean, 10th and 90th percentile: a) bottom temperature (position A), b) core temperature (position B) and c) surface temperature (position C). The 500 Monte Carlo simulations are shown in grey.

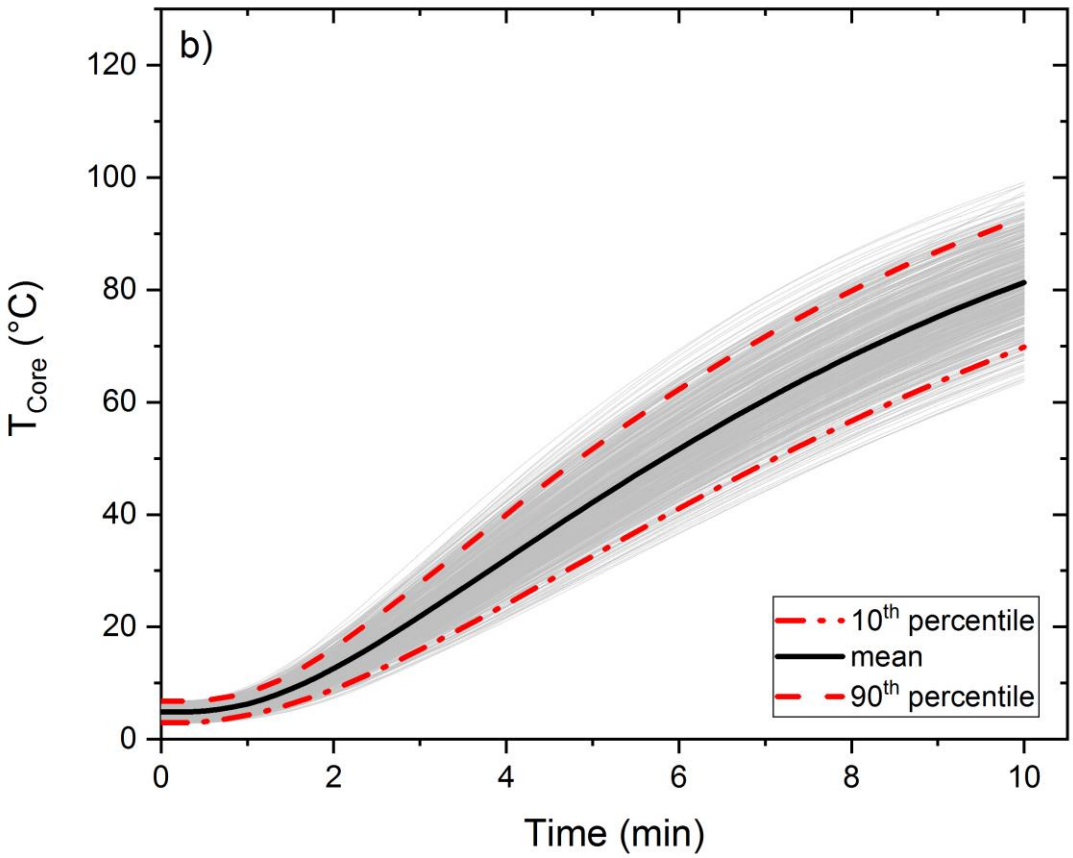

Figure 2: Uncertainty of the predicted temperature development using mean, 10th and 90th percentile: a) bottom temperature (position A), b) core temperature (position B) and c) surface temperature (position C). The 500 Monte Carlo simulations are shown in grey.

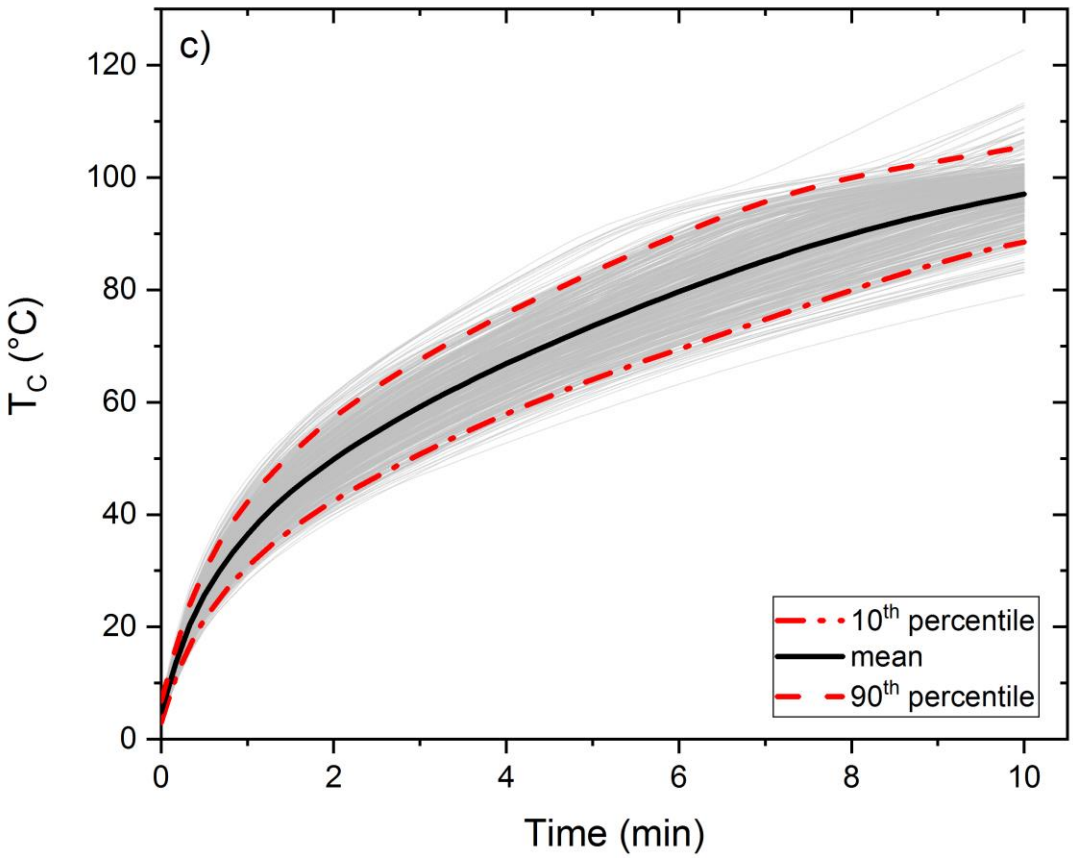

Figure 2: Uncertainty of the predicted temperature development using mean, 10th and 90th percentile: a) bottom temperature (position A), b) core temperature (position B) and c) surface temperature (position C). The 500 Monte Carlo simulations are shown in grey.

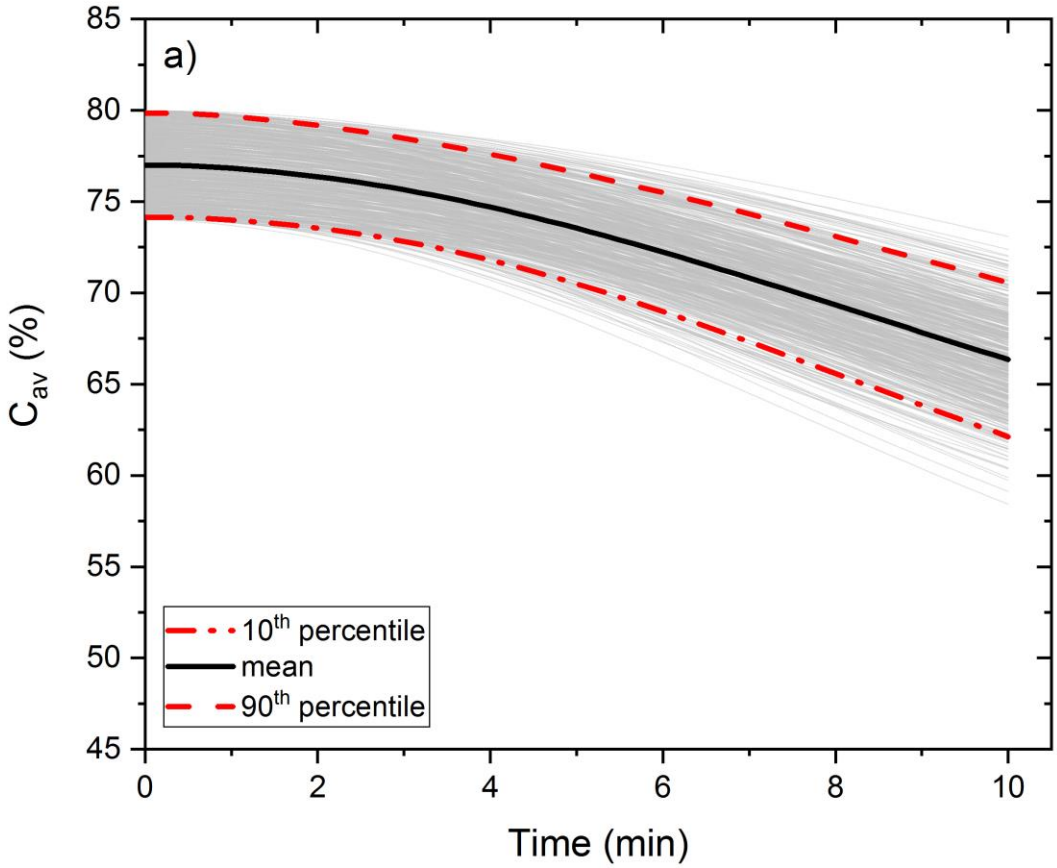

Figure 3: Uncertainty of the predicted moisture content development using mean, 10th and 90th percentile: a) average moisture content, b) moisture content close to the bottom (position A) and c) moisture content close to the surface (position C). The 500 Monte Carlo simulations are shown in grey.

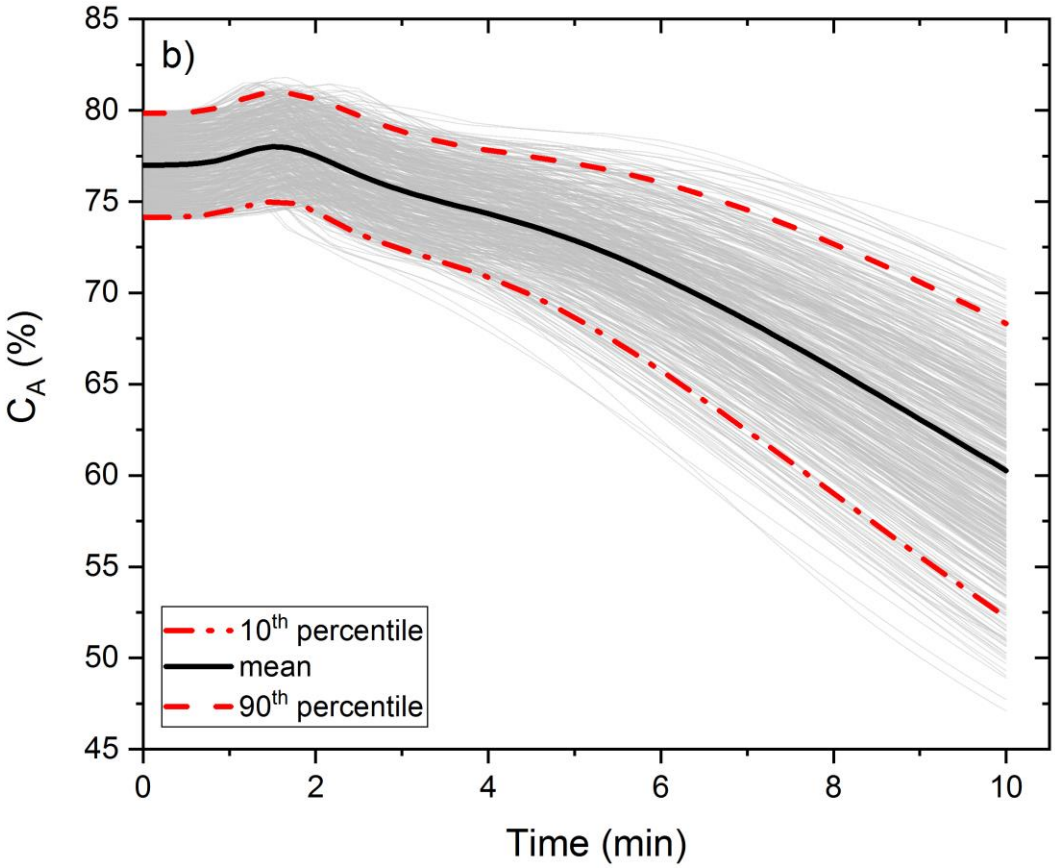

Figure 3: Uncertainty of the predicted moisture content development using mean, 10^{th} and 90^{th} percentile: a) average moisture content, b) moisture content close to the bottom (position A) and c) moisture content close to the surface (position C). The 500 Monte Carlo simulations are shown in grey.

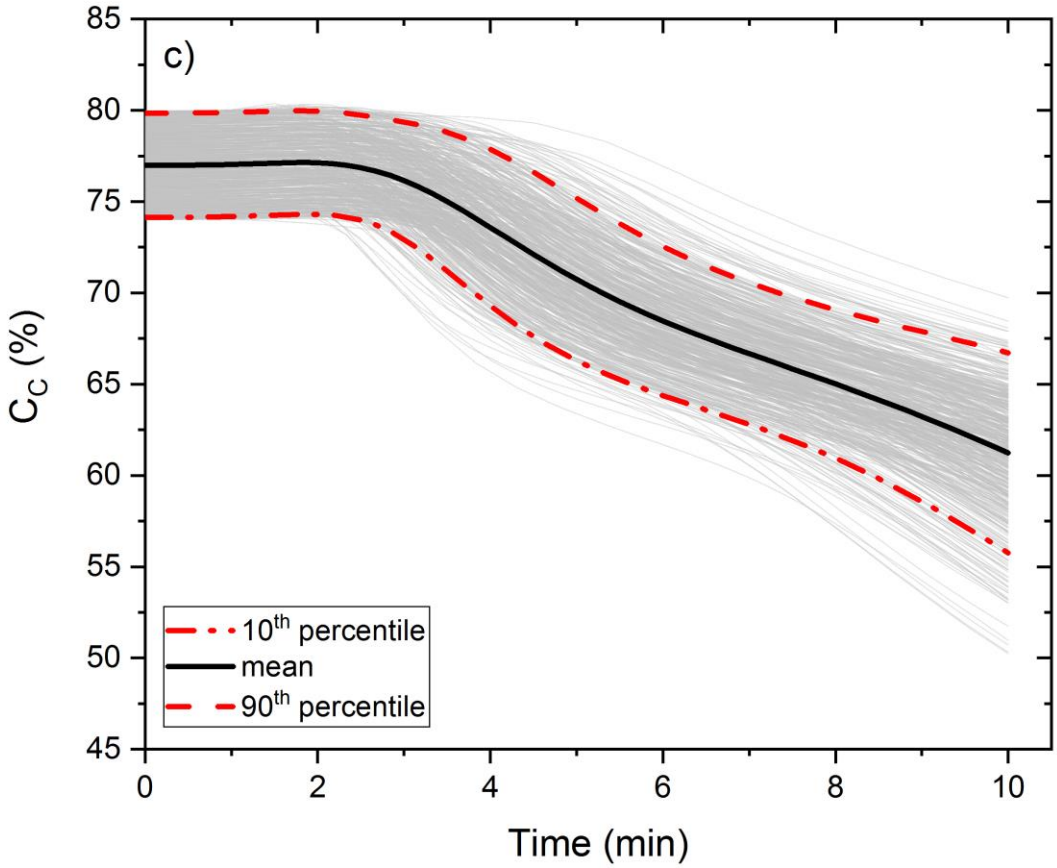

Figure 3: Uncertainty of the predicted moisture content development using mean, 10th and 90th percentile: a) average moisture content, b) moisture content close to the bottom (position A) and c) moisture content close to the surface (position C). The 500 Monte Carlo simulations are shown in grey.

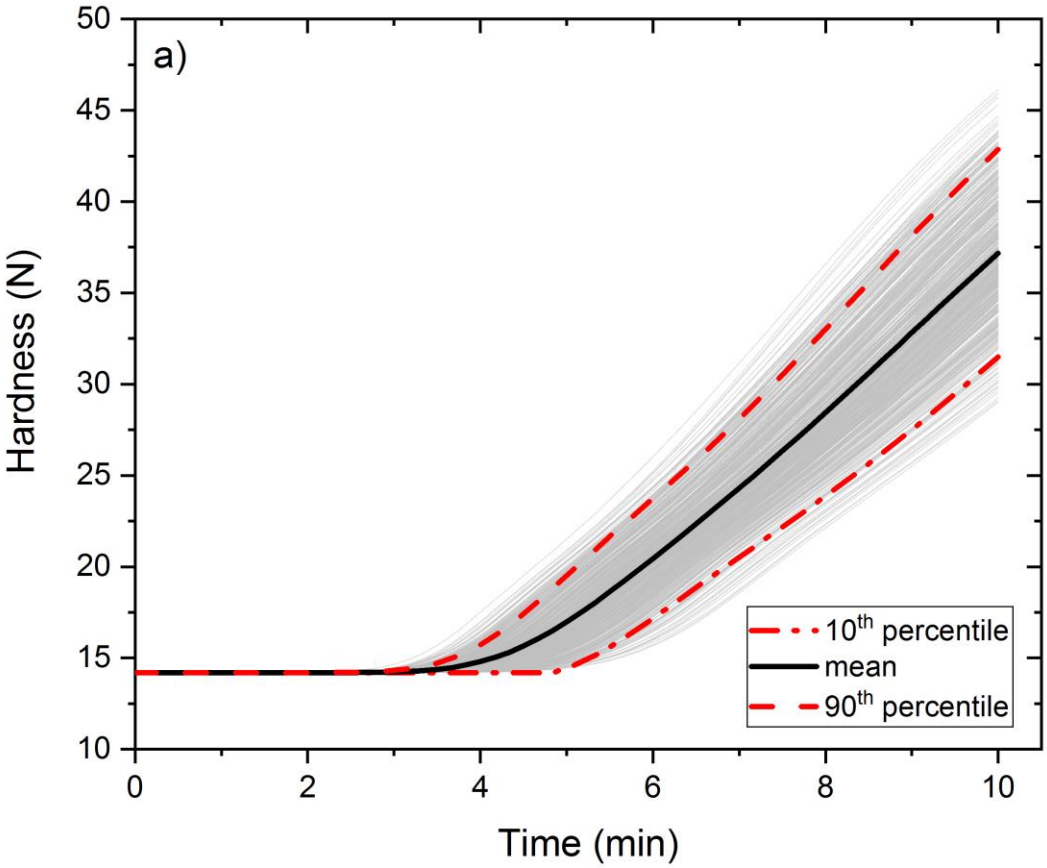

Figure 4: Uncertainty of the predicted development of the texture parameters a) hardness (*Ha*) and b) chewiness (*Cw*) using mean, 10th and 90th percentile. The 500 Monte Carlo simulations are shown in grey.

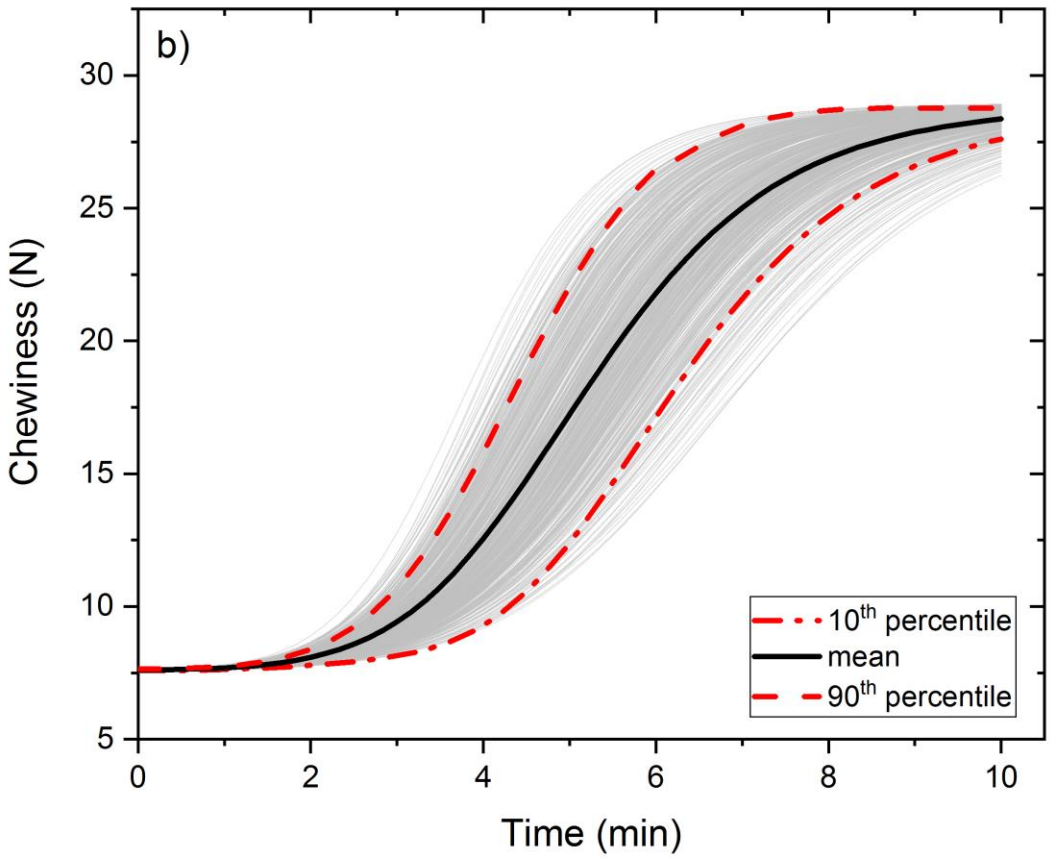

Figure 4: Uncertainty of the predicted development of the texture parameters a) hardness (*Ha*) and b) chewiness (*Cw*) using mean, 10th and 90th percentile. The 500 Monte Carlo simulations are shown in grey.

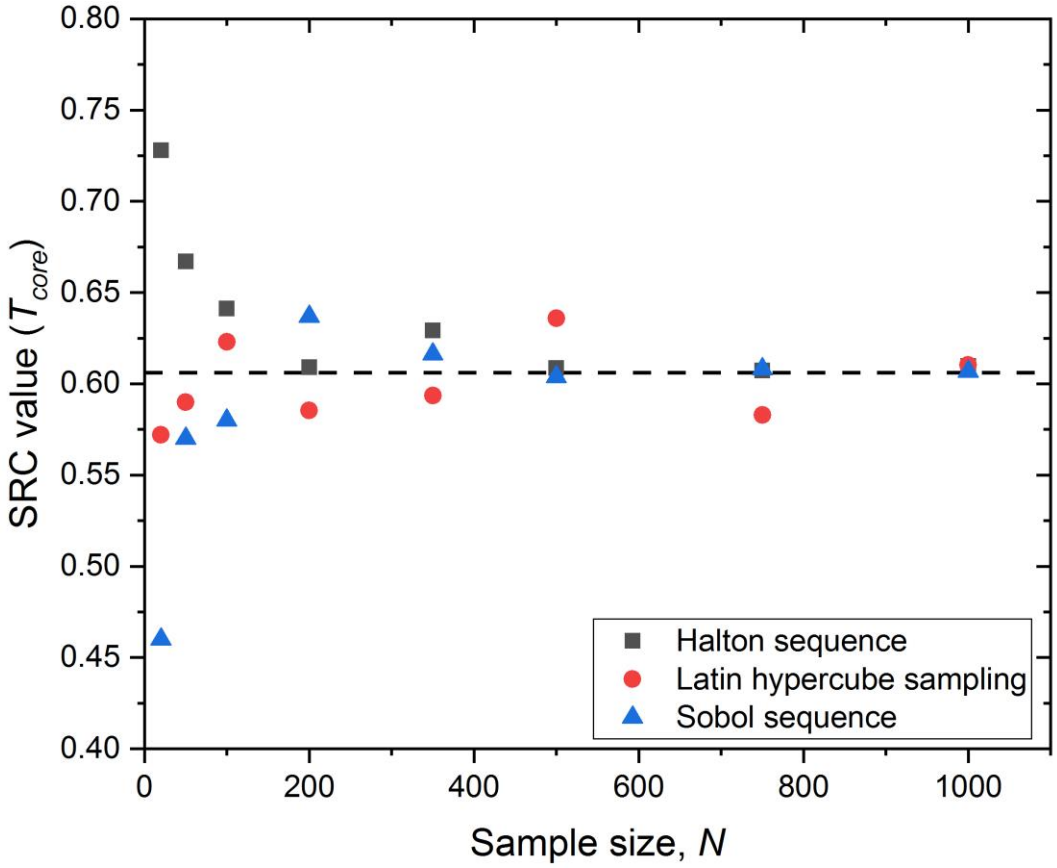

Figure 5: Influence of the different sampling methods (Latin hypercube sampling, Halton sequence and Sobol sequence) and the sampling size on the resulting SRC value (input parameter: oven temperature T_{oven}; output variable: core temperature T_{core}) at the roasting time of 8 min. The dashed line shows the mean SRC value after 1000 simulations using the Halton sequence.

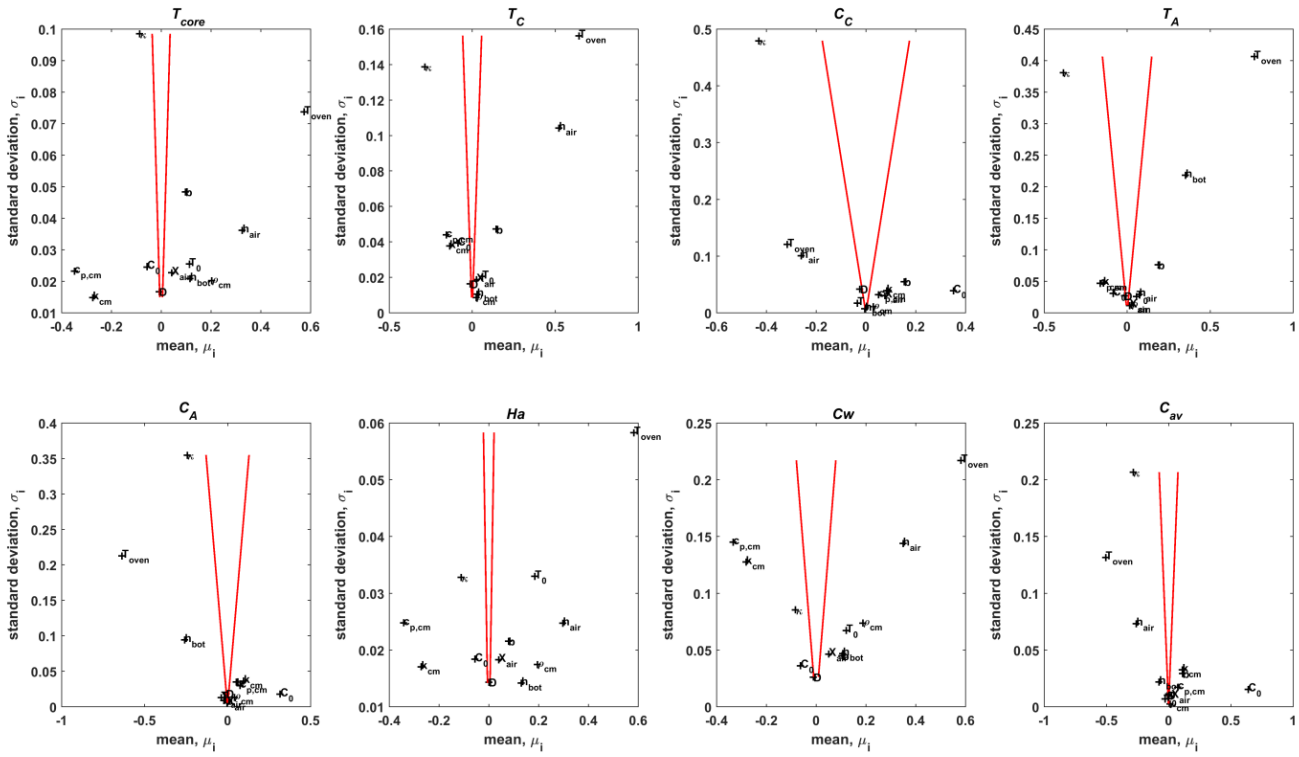

Figure 6: Mean (μ_i) and standard deviation (σ_i) of the Elementary Effects distribution of the model input parameters (in total 12 parameters symbolized as crosses with names) on the model outputs. The two lines in each of the plots correspond to $\mu_i = \pm 2sem_i$.

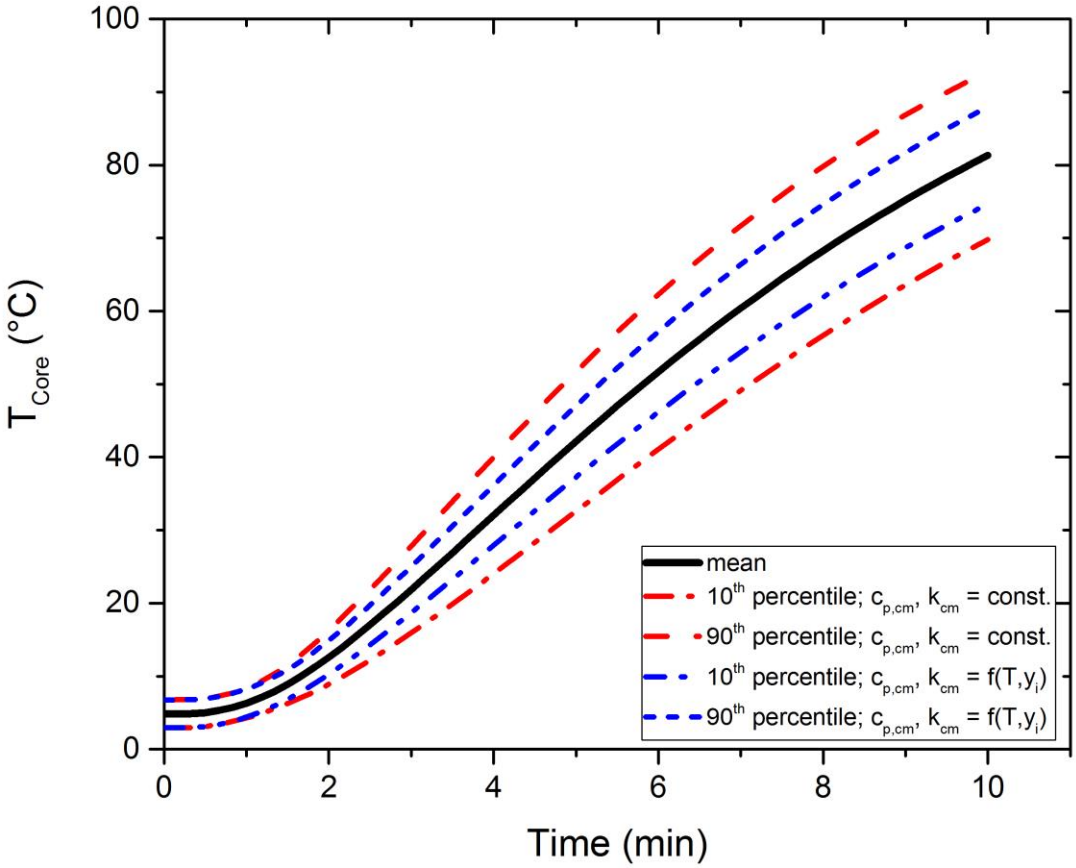

Figure 7: Uncertainty of the predicted temperature development at the core with fixed values of $c_{p,cm}$ and k_{cm} (red dashed lines) and with $c_{p,cm}$ and k_{cm} as function of temperature and composition (blue dashed lines).

Highlights:

- Global uncertainty and sensitivity analysis is a strong tool in complex food processes
- The mechanistic 3D model of chicken meat roasting was evaluated
- The uncertainty in the model predictions were obtained with the Monte Carlo method
- The most influencing model input parameters were identified and ranked accordingly
- The benefit of the analysis was illustrated by using the result for model refinement